Published in final edited form as:

Cell Death Differ. 2009 August ; 16(8): 1108–1117. doi:10.1038/cdd.2009.25.

The alpha/beta carboxyterminal domains of p63 are required for skin and limb development. New insights from the Brdm2 mouse which is not a complete p63 knockout but expresses p63 gamma-like proteins

Sonja Wolff[1,*], **Flaminia Talos**[2,*], **Gustavo Palacios**[2], **Ulrike Beyer**[1], **Matthias Dobbelstein**[1], and **Ute M. Moll**[1,2]

[1]Dept. of Molecular Oncology, University of Göttingen, 37077 Göttingen, Germany

[2]Dept. of Pathology, Stony Brook University, Stony Brook, NY 11794-8691, USA

Abstract

p63, an ancestral transcription factor of the p53 family, has three C-terminal isoforms whose relative *in vivo* functions are elusive. The p63 gene is essential for skin and limb development, as vividly shown by two independent global knockout mouse models. Both strains, although constructed differently, have identical and severe phenotypes, characterized by absent epidermis and hindlimbs and only rudimentary forelimbs at birth. Here we show that mice from one model, Brdm2, express normal levels of truncated p63 proteins that contain the DNA binding and oligomerization domain but lack the long carboxy-terminal SAM (sterile α-motif) and post-SAM domains that are specific for the α and β isoforms. As such, transcriptionally active p63 proteins from Brdm2 mice resemble the naturally occurring p63γ isoforms, which of all p63 isoforms most closely resemble p53. Thus, Brdm2 mice are p63α/β isoform-specific knockout mice, gaining unexpected new importance. Our studies identify that p63α/β but not p63γ are absolutely required for proper skin and limb development.

Keywords

p63; p63 C-terminal isoforms; skin and limb development

Introduction

The transcription factor p63, a member of the p53 family and in parts a structural homolog, plays a pivotal role in epidermal and limb development, as shown by two mouse models. The p63 gene consists of 14 Exons and produces 6 well described isoforms, derived from two promoters (TA and ΔN) that each give rise to three different carboxytermini via alternative splicing. The longest α isoform skips Exon 10′ (originally called Exon 15, see

Correspondence and requests for materials should be addressed to U.M.M. (umoll@notes.cc.sunysb.edu)..

*These authors contributed equally to this work.

Genbank Accession Nr. AF533892), the β isoform skips Exon 13 and the γ isoform ends with alternatively spliced Exon 10′ 1.

Soon after the gene's discovery, two groups generated p63 knockout models but used different embryonic stem cell ablation technologies for p63 exon disruption 2,3. McKeon and colleagues replaced Exons 6-8 in the DNA binding domain (which is common to both TA and ΔN isoforms) with a Neo cassette, leading to a complete loss of all p63 proteins. In contrast, Mills and colleagues employed a gap-repair mechanism for p63 targeting, using an insertional vector from a pre-existing library 4. In the Mills *et al* mutant allele named Brdm2 2, the target vector insertion interrupted the gene only after Exon 10, followed by a net duplication of the region of homology (Exons 5-10), plus the endogenous Exons 10′-14 (Figure 1a). Importantly, the phenotypes of both homozygous mutant models are identical and dramatic: newborns with essentially no epidermis nor epidermal appendages, absence of hind limbs, only rudimentary forelimbs, craniofacial abnormalities, and profound defects in other stratified epithelial tissues (urothelium, mammary and prostate) 2,3. In contrast, heterozygous mice for either of these mutations showed none of these phenotypes 2,3.

Nevertheless, over the ensuing years both KO models have generated a vexing degree of disagreement that remain unresolved 5. Examples include the role of p63 in skin epithelial commitment and terminal differentiation *versus* stem cell proliferation 5-7 and in oncogenic *versus* tumor suppressor function in tumorigenesis 8-10. Of note, by far most studies on p63 function were performed on the Brdm2 strain 2,6,8,9,11-24, from which major conclusions were drawn about its role in developmental neuronal apoptosis 14, in germ cell apoptosis during testicular development and irradiation 19,22,23 and in organismal senescence during aging 15.

Results

Brdm2 embryos express normal levels of truncated p63 proteins that contain the DNA binding and oligomerization domain but lack the long carboxy-terminal SAM and post-SAM domains

For unrelated studies we needed p63 null tissues. Genotyping of Brdm2/Brdm2 mice (gift of A. Mills) across the p63 genomic/vector border invariably confirmed the reported insertion of the targeting vector between Exon 10 and 10′ in all embryos studied (Figure 1a) 2. A total of 26 Brdm2/Brdm2 embryos were examined, ranging from day E13 to P1 newborns. Phenotypes were invariant. As expected 2,3, by macroscopic inspection, late stage E18 Brdm2/Brdm2 embryos (called B/B in Figures) exhibited a profound lack of epidermis, absent hindlimbs and severely underdeveloped forelimbs (Figure 1b). In contrast, p63 wild-type (WT) and heterozygous (WT/Brdm2, data not shown) littermates exhibited well developed limbs and epidermis (Figure 1b), with p63 expression in nuclei of basal and suprabasal cells of skin and hair follicles (Figure 1c, d). This was readily detectable by the classic monoclonal pan-p63 antibody 4A4 that detects all isoforms. The apical ectodermal ridge in WT but not p63-/- limb buds also expresses high levels of p63 protein 3. Microscopically, mutant E18 Brdm2/Brdm2 embryos were essentially devoid of epidermis, exposing only compressed dermis (Figure 1e, f). However, close inspection revealed rare patches of keratinizing epidermis with relatively normal squamous stratification overlying

hair follicles (Figure 1e, f). Unexpectedly, these patches expressed high levels of nuclear p63 in basal and suprabasal cells, comparable to WT tissue (Figure 1f). Moreover, in mechanically protected anatomic niches like the anterior nasal cavity (Figure 1g, h) and the buccal mucosa of the oral cavity of mutant mice (Figure 2a, b), well-developed fragments of normal appearing non-keratinizing squamous epithelium were present. These areas also expressed p63 at WT levels (Figure 1h and Figure 2b). Furthermore, p63 was strongly expressed in cell nuclei of the anterior pituitary as well as gonocytes of testis and ovary of Brdm2/Brdm2 mice (Figure 2c, d and data not shown). To confirm this completely unexpected p63 expression in mutant Brdm2/Brdm2 mice, we validated the p63 specificity of the 4A4 antibody which was raised against aa 1-205 of ΔNp63, spanning the end of Exon 3′ to the start of Exon 7 within the DNA binding domain 1. First, remnant epidermal patches and internal squamous and stratified mucosa in McKeon p63 KO mice 3 at day E17 did not yield any 4A4 staining (Figure 3a, b and data not shown).

Moreover, specific pre-absorption with lysates of H1299 cells transfected with a 1:1 mixture of TAp63α and ΔNp63α expression plasmids abolished or severely reduced nuclear 4A4 staining (Figure 3c,d), while pre-absorption with empty vector lysates did not (Figure 3e). Also, when 4A4 was omitted, immunostaining was lost (data not shown). Finally, 4A4 recognizes the same specific cell types (basal keratinocytes, squamous carcinoma cells, neurons, urothelium, breast and prostate) - and no other - in mouse and human tissues, where it has become a clinically validated diagnostic antibody for p63 (e.g. Ref 24) (Figure 3f, g and data not shown). Together, these data confirm the exclusive specificity of the 4A4 antibody for p63 and further excludes any possible cross-reactivity with p53 family members in skin and other stratified epithelia. To further confirm p63 expression in Brdm2/Brdm2 embryos, we used a second independent anti-p63 antibody, polyclonal H-137 raised against aa 15-151 of ΔNp63. As expected, H-137 immunostained epidermis and internal epithelia in WT E18 embryos (Figure 3h and data not shown). Of note, H-137 also immunostained epidermis and internal epithelia in Brdm2/Brdm2 embryos in a pattern identical to the one seen with 4A4 (Figure 2 l-m and data not shown).

We rationalized that the squamous patches in mutant E18 Brdm2/Brdm2 embryos might be surviving remnants of a better developed epidermis from an earlier stage. E15 is the developmental stage when commitment to terminal differentiation occurs 16. Indeed, while the limb truncation phenotype of E15 Brdm2/Brdm2 embryos was already fully evident, they exhibited a thin and translucent but widely intact epidermal integument when closely inspected with a dissecting microscope (Figure 1i; note: the photograph does not capture the image seen by eye). The presence of an albeit thin but intact integument at E15 was confirmed microscopically (Figure 1j, n). The E15 mutant epidermis consists of a largely contiguous, terminally differentiated keratinizing squamous epithelium that is 3-5 cell layers thick, with focal thickening (Figure 1j, m) and patchy underlying hair follicles (Figure 1k, l). Importantly, the mutant epidermis strongly expresses nuclear p63 in an orderly row of basal progenitors and suprabasal keratinocytes, with a p63 distribution and staining intensity similar to that of WT epidermis (Figure 1k-n). Moreover, the internal stratified squamous mucosa covering tongue, buccal areas, oropharynx and nasopharynx, esophagus, forestomach and bladder was invariably well developed by H&E and stained strongly positive for p63 with both monoclonal 4A4 and polyclonal H-137 antibodies (Figure 2e-m).

Thus, indeed, the epithelializations of E18 Brdm2/Brdm2 embryos appear to be remnants of a better developed epithelium at stage E15, which, importantly, is of a transient nature. Future work focusing on the role of p63 in epithelial stemness and/or adhesion will clarify why the embryonic epidermis is well formed at day E15 but disappears at later stages in these mutant embryos.

To further support p63 protein expression in mutant Brdm2/Brdm2 animals, we performed quantitative RT-PCR analysis in E15 embryos and mouse embryo fibroblasts (MEFs) derived from E13 embryos. Multiple p63 transcripts derived from Exon 1 to Exon 10 (including TA and ΔN variants) were readily detectable in amounts comparable to that of wild-type mice when normalized for either GAPDH, β-actin or the ribosomal protein Rplp0, present in all tissues (Figure 4b-d and data not shown, summarized in Figure 4a). p63 expression was also normalized to skin markers. These were present at 6 to 8-fold lower levels in mutant embryos, confirming the visual skin impression (see Figure 1i). Indeed, when p63 transcript levels were normalized for multiple epidermal differentiation markers such as cytokeratin K5 and K14 (basal cell layer), K10 (intermediate layer), loricrin (top layer) and desmosomal marker PERP (all layers), on the whole these broad-based normalizations showed that mutants expressed levels of p63 Ex1-10 that were comparable to those of WT (Figure 4b, Supplemental Figure 1 and data not shown). In contrast, p63 Ex4-Ex10′ and Ex4-Ex11 transcripts were only detected in WT but never in Brdm2/Brdm2 embryos (Figure 4b). Thus, transcription from the Brdm2 allele occurs from Exon 1-10 but does not cross the vector insert. Instead, two novel transcripts extending from Exon 10 are readily detectable in Brdm2/Brdm2 embryos at day E15. Both are missing the 37 amino acid tail of p63γ encoded by Exon 10′ and the extensive carboxytermini of p63α and β encoded by Exons 11-14. One transcript is a read-through from Ex10 into the adjacent Intron 10, forming an open reading frame that is then immediately terminated by a stop codon after only 1 nucleotide into Intron 10. The other is the result of splicing Exon 10 in frame onto the nonfunctional 3′ portion of the *hprt* minigene (Figure 4a). The 3′*hprt* cassette has a splice acceptor site at its 5′ end and is followed by its 3′UTR (Figs. 1a and 4a). 3′ RACE and sequencing further confirmed the presence of both novel transcripts exclusively in Brdm2/Brdm2 embryos. These truncated transcripts were apparently missed in the original study using Northern blots that detected long 5 kb mRNA species from the p63 wild-type allele 2, possibly because they are much smaller than the bona fide p63α mRNAs. Taken together, the invariant presence of the targeting vector after Exon 10 at the reported location (Figure 1a, Mills et al. 1999), the absence of wild-type RT-PCR products that span the vector insertion (Ex 4-10′ and Ex 4-11) in Brdm2/Brdm2 embryos (Figure 4b), and the reproducibility of the Brdm2/Brdm2 phenotype in random litters exclude the pro forma possibility of an accidental reversion to a wild-type p63 gene by spontaneous excision of targeting vector plus its duplicated Ex5-10.

Transcriptionally active p63 proteins from Brdm2 mice resemble the naturally occurring p63γ isoforms

Immunoblots showed that the recombinant Brdm2 Ex10-truncated p63 proteins, TA(1-10) and ΔN(3′-10), have the same steady state levels as the respective native mouse p63γ. In contrast, Hprt fusion proteins of TA(1-10) and ΔN(3′-10) are unstable (Figure 5a). To test

the function of Brdm2 p63 proteins, we performed Luciferase reporter assays using the p53/p63-responsive human Mdm2 promoter P2 as driver 13 and compared their activities to bona fide mouse p63γ. In sum, TA(1-10) and ΔN(3′-10) behave indistinguishably from genuine p63γ. Specifically, in transactivation assays TA(1-10) was at least as active as native TAp63γ (Figure 5b), while both ΔN(3′-10) and ΔNp63γ exhibited only minimal transactivation (Figure 5c). The respective p63-Hprt fusions were inactive in transactivation (Figure 5b, c bottom). Likewise, in competitive transrepression assays using either p53 or TAp63γ as the activity to be suppressed, ΔN(3′-10) and ΔNp63γ again behaved indistinguishably (Figure 5d). On the other hand, ΔN(3′-10)Hprt fusion was equally repressive towards p63, but less so towards p53 (Figure 5d). Given that mixed tetramers between wild-type p53 and p63 proteins do not form 12 but p63 homotetramers do, we speculate that this reflects the fact that the bulky Hprt tag might impair direct DNA binding of ΔN(3′-10)Hprt homotetramers, while it still allows to engage in mixed tetramers with TAp63γ, thereby acting as a stronger dominant negative. At any rate, since it is unclear whether Hprt fusions are stable *in vivo*, it suggests that the latter Brdm2 protein plays either no or only a minor role.

To further validate these results, we performed immunoblot analysis on tissue lysates obtained from the snout and mouth region of WT and Brdm2/Brdm2 E15 littermates and compared them with corresponding lysates of McKeon p63 KO E15 embryos. The results show a unique and reproducible band in Brdm2/Brdm2 embryos that aligns with transfected p63Ex10-truncated ΔN(3′-10) control protein and is absent in WT and p63 KO embryos (Supplemental Figure 2). Taken together, we propose that the strong specific p63 immunostaining present in mutant skin and squamous epithelium (Figures 1 and 2) is largely due to p63Ex10-truncated ΔN(3′-10) and to a lesser extent to TA(1-10) proteins.

Next we assessed whether the Brdm2 proteins have p63γ-like transcriptional activity *in vivo*. Previously it was shown that the absence of p63 results in a strong reduction of CK14 and PERP, identifying these genes as important bona fide epidermal target genes of p63γ 25-27. CK14 is a marker of the basal layer of stratified epithelia, while PERP, a component of desmosomes which are specialized intraepithelial cell-cell adhesion junctions, is expressed in all cell layers of the epidermis. Importantly, indeed, both CK14 and PERP proteins were expressed in Brdm2/Brdm2 E15 skin at wild-type levels, thus confirming the *in vivo* functionality of Brdm2 proteins (Figure 6). In sum, our protein expression, RT-PCR and functional *in vitro* and *in vivo* data prove that the Brdm2 allele is not a null allele, as had been assumed all along in a series of previous studies using the Brdm2 mouse model (see References 2,6,8,11-24,29), but generates ΔN and TA variants of truncated p63 proteins that structurally and functionally resemble the native p63γ isoforms. Moreover, our data provide further biological and functional insight into the role of the long carboxyterminal domain of p63 in skin and limb development.

Discussion

Brdm2 mice are p63α/β isoform-specific knockout mice, gaining unexpected new importance

The skin and limb phenotype of both strains of targeted p63 mice that were generated 9 years ago to ablate the entire p63 gene is identical at birth 2,3. Our results shed new and unexpected light on one of the two strains, the heavily used Brdm2 mice. Instead of being a global p63 KO model, we show that as a consequence of the 'late' insertion of the targeting vector only after Exon 10, they are in fact p63α/β isoform-specific knockouts that express p63γ-like proteins at quasi wild-type levels. Thus, the dramatic phenotype of the mutant mice is entirely attributable to the absence of the carboxyterminal tail present in p63α/β. With this reinterpretation Brdm2 mice take on unexpected new importance. They positively map the p63 region required for skin and limb development to Exons 11-14, which encode the functionally important SAM and post-SAM domains. Both domains are specific for p63α but not γ isoforms and absent in p53. In strong support of the importance of the SAM and post-SAM domains in ectodermal and limb development are the human ectodermal dysplasia syndromes of ankyloblepharon-ectodermal dysplasiaclefting, i.e. the Hay-Wells and related syndromes. These congenital abnormalities of limbs, skin, hair, teeth, nails and palate are due to various heterozygous point mutations within the SAM and post-SAM domains of human p63 20,21. Moreover, although ΔNp63α appears to be the predominant isoform expressed in mature stratified epithelia 1, it was unknown whether α isoforms are essential or if other isoforms can substitute for α in epithelial and limb development and homeostasis. Our results show that the carboxyterminal domains of p63 are indeed required for the full morphogenetic program of skin and limb development, and likely also for maintenance of mature skin. The p63γ isoform thus allows to set up embryonic epidermal fate, while the α/β isoform is necessary for skin homeostasis. p63γ-like isoforms cannot substitute for p63 α/β in these tissues (nor can p53 which is present in Brdm2 mice).

Furthermore, our findings make it necessary to reinterpret other previous results using Brdm2 mice. Any phenotype that was observed with this mouse strain is due to a selective loss of long p63 isoforms. Thus, previous studies on the development of urogenital 11,17,18,30-32, gonadal 19,22,23 and sympathetic neuronal systems 14 may have addressed the biological consequences of tipping the balance between full-length and carboxyterminally truncated p63, rather than the effect of losing all p63 isoforms.

Finally, our results reconcile at least in part some unresolved controversies in the p63 field. Different conclusions may now be linked to the use of the two different KO models 2,3 that, as shown here are not interchangeable, but represent a complete KO 3 in contrast to a p63α/β isoform-specific KO 2. One example is the controversial function of p63 in skin, assigning it an essential role in proliferation of skin stem cells 3,7 *versus* a role in terminal differentiation 2,16. In another example, Brdm2 heterozygotes were not prone to or even protected from spontaneous or genotoxically induced tumors compared to their WT counterparts 8,9, which was interpreted as evidence that the p63 gene functions as an oncogene by virtue of repressing the tumor suppressive mechanisms of cellular senescence 9,33. This result contrasted with evidence for a p63 tumor suppressor function obtained in

spontaneous tumorigenesis studies with the complete p63KO strain 10. In light of our findings here, some conclusions about p63′s protective role in tumorigenesis might have to be reexamined. The exclusively expressed p63γ-like proteins in Brdm2 mice have transactivation and transrepression activities comparable to p63γ and could conceivably act similar to p53-like tumor suppressors, providing cancer protection. Future studies will need to define the exact functions of the p63α/β carboxyterminal domains in development and tumorigenesis. Brdm2 mice will be a valuable tool in this endeavour.

Materials and Methods

Mice

Genotyping of p63 Brdm2/Brdm2 mice (maintained as C57Bl6/129 50:50; also available as JAX Mice # 003568) across the p63 genomic/vector border confirmed the reported insertion of the targeting vector between Exon 10 and Exon 10′ 2. The gap-repair mechanism leads to a duplication of Exons 5-10. A forward primer in Intron 10 (gtgttggcaaggattctgagacc, nt 187617-187639, Genbank AF533892) and a reverse primer located in the targeting vector pTV12E60 (cloning vector pIRES1neo, Genbank U89673.1) (ggaagacaatagcaggcatgct, nt 2672-3128) yields a 410 bp product which maps as indicated by the red line in Figure 1a. p63 knockout mice (Yang A et al, 1999) were a gift from F. McKeon and G. Melino.

Histological analysis and immunoperoxidase staining

Embryos were fixed in 10% buffered formalin, dehydrated, embedded in paraffin, and sectioned at 4 μm thickness. Sections were dewaxed, rehydrated, and stained in hematoxylin and eosin. Immunoperoxidase staining with p63-specific monoclonal antibody 4A4 was performed using a standard protocol. Briefly, for antigen retrieval deparaffinized slides were boiled in citric acid buffer (10 mM, pH 6.0) in a microwave 2 × 5 min, (alternatively for H-137 with Trilogy, Cell Marque, CA), washed in PBS, quenched in 1% H_2O_2 for 15 min, washed and blocked with 10% serum for 20 min (Histostain SP Broad Spectrum HRP kit, ZYMED). Sections were incubated with either 4A4 IgG (Santa Cruz, diluted 1: 200 in 2% blocking serum), H-137 (Santa Cruz, diluted 1:100), anti-cytokeratin 14 (CK14) (gift of Alea Mills) or anti-PERP specific antibody (gift of Laura Attardi) for 1-2 hrs at room temperature (RT) or at 4°C overnight. After washing 3 times in PBS, sections were incubated in biotinylated secondary antibody for 45 min at RT, washed and incubated with Streptavidin-HRP prior to development with diaminobenzidine for 10 min, followed by dehydration and coverslipping.

Quantative real-time reverse transcription PCR (qRT-PCR)

Total RNA was isolated from WT and Brdm2 E15 embryos or low passage MEFs using PureLink (Invitrogen). RNA was reverse transcribed using the iScript cDNA Synthesis Kit (BioRad) according to manufacturer's instructions. IQ SYBR Green Supermix (BioRad) was used for real-time PCR applications. The primer sets are listed in Supplemental Table S1. PCR conditions were: 2 min at 95°C, followed by 40 cycles of 95°C for 15 sec, 58-62°C for 30 sec, and 72°C for 30-120 sec. p63 transcript levels were normalized to GAPDH or loricrin (Figure 4b), calculated using the 2- ΔΔCt method.

Cloning of expression plasmids

cDNAs of all Brdm2 allele-derived p63 products were amplified by PCR, sequence confirmed and inserted into pCDNA3. Mouse TAp63γ, ΔNp63γ and p53 were also cloned into pcDNA3.

Immunoblots

Total cell lysates (20 μg) were separated on SDS-polyacrylamide gels and transferred to nitrocellulose, followed by incubation with 4A4 antibody (1:500 in PBS containing 5% milk powder and 0.05% Tween 20). Detection was performed by a peroxidase-coupled secondary antibody (Jackson) and ECL chemiluminescence (Pierce).

Luciferase assays

H1299 cells (1×10^5 cells/well) were transfected with Lipofectamine 2000 in duplicates with 100 ng of BP100luc and 50 ng of renilla reporters. To compensate for the instability of Hprt-fusion proteins, amounts of the indicated p63 expression plasmids were adjusted to achieve equal protein expression, as shown by 4A4 immunoblots (Figure 5b, d, f; 20 μg lysates each). For assessment of transactivation (Figure 5c, e), p63 plasmids were 25 ng of mouse TAp63γ and TA(1-10), and 50 ng TA(1-10)Hprt (Figure 5c), or 12.5 ng mouse ΔNp63γ and ΔN(3′-10), and 75 ng ΔN(3′-10)Hprt (Figure 5e). For assessment of transrepression of TAp63γ (25 ng plasmid) or p53 (5 ng plasmid) (Figure 5g, h), ΔNp63 expression plasmids were transfected in excess (8-fold each of ΔNp63γ and ΔN(3′-10) and 48-fold of ΔN(3′-10)Hprt plasmids) with respect to TAp63γ to achieve equal transrepressor protein levels (Figure 5f). Values were normalized for renilla.

Supplementary Material

Refer to Web version on PubMed Central for supplementary material.

Acknowledgments

We thank A. Mills for providing Brdm2 mice and for critical reading and discussion of the manuscript. This work was supported by the National Cancer Institute (U.M.M), the Carol Baldwin Breast Cancer Award (U.M.M), the Deutsche Krebshilfe (U.M.M.), and the Deutsche Forschungsgemeinschaft (M.D.).

References

1. Yang A, Kaghad M, Wang Y, Gillett E, Fleming MD, Dotsch V, et al. p63, a p53 homolog at 3q27-29, encodes multiple products with transactivating, death-inducing, and dominant-negative activities. Mol Cell. 1998; 2:305–316. [PubMed: 9774969]
2. Mills AA, Zheng B, Wang XJ, Vogel H, Roop DR, Bradley A. p63 is a p53 homologue required for limb and epidermal morphogenesis. Nature. 1999; 398:708–713. [PubMed: 10227293]
3. Yang A, Schweitzer R, Sun D, Kaghad M, Walker N, Bronson RT, et al. p63 is essential for regenerative proliferation in limb, craniofacial and epithelial development. Nature. 1999; 398:714–718. [PubMed: 10227294]
4. Zheng B, Mills AA, Bradley A. A system for rapid generation of coat color-tagged knockouts and defined chromosomal rearrangements in mice. Nucleic Acids Res. 1999; 27:2354–2360. [PubMed: 10325425]
5. McKeon F. p63 and the epithelial stem cell: more than status quo? Genes Dev. 2004; 18:465–469. [PubMed: 15037544]

6. Koster MI, Kim S, Mills AA, DeMayo FJ, Roop DR. p63 is the molecular switch for initiation of an epithelial stratification program. Genes Dev. 2004; 18:126–131. [PubMed: 14729569]
7. Senoo M, Pinto F, Crum CP, McKeon F. p63 Is essential for the proliferative potential of stem cells in stratified epithelia. Cell. 2007; 129:523–536. [PubMed: 17482546]
8. Perez-Losada J, Wu D, DelRosario R, Balmain A, Mao JH. p63 and p73 do not contribute to p53-mediated lymphoma suppressor activity in vivo. Oncogene. 2005; 24:5521–5524. [PubMed: 16007185]
9. Keyes WM, Vogel H, Koster MI, Guo X, Qi Y, Petherbridge KM, et al. p63 heterozygous mutant mice are not prone to spontaneous or chemically induced tumors. Proc Natl Acad Sci U S A. 2006; 103:8435–8440. [PubMed: 16714381]
10. Flores ER, Sengupta S, Miller JB, Newman JJ, Bronson R, Crowley D, et al. Tumor predisposition in mice mutant for p63 and p73: evidence for broader tumor suppressor functions for the p53 family. Cancer Cell. 2005; 7:363–373. [PubMed: 15837625]
11. Cheng W, Jacobs WB, Zhang JJ, Moro A, Park JH, Kushida M, et al. DeltaNp63 plays an anti-apoptotic role in ventral bladder development. Development. 2006; 133:4783–4792. [PubMed: 17079275]
12. Davison TS, Vagner C, Kaghad M, Ayed A, Caput D, Arrowsmith CH. p73 and p63 are homotetramers capable of weak heterotypic interactions with each other but not with p53. J Biol Chem. 1999; 274:18709–18714. [PubMed: 10373484]
13. Freedman DA, Epstein CB, Roth JC, Levine AJ. A genetic approach to mapping the p53 binding site in the MDM2 protein. Mol Med. 1997; 3:248–259. [PubMed: 9131587]
14. Jacobs WB, Govoni G, Ho D, Atwal JK, Barnabe-Heider F, Keyes WM, et al. p63 is an essential proapoptotic protein during neural development. Neuron. 2005; 48:743–756. [PubMed: 16337913]
15. Keyes WM, Wu Y, Vogel H, Guo X, Lowe SW, Mills AA. p63 deficiency activates a program of cellular senescence and leads to accelerated aging. Genes Dev. 2005; 19:1986–1999. [PubMed: 16107615]
16. Koster MI, Dai D, Marinari B, Sano Y, Costanzo A, Karin M, et al. p63 induces key target genes required for epidermal morphogenesis. Proc Natl Acad Sci U S A. 2007; 104:3255–3260. [PubMed: 17360634]
17. Kurita T, Cunha GR, Robboy SJ, Mills AA, Medina RT. Differential expression of p63 isoforms in female reproductive organs. Mech Dev. 2005; 122:1043–1055. [PubMed: 15922574]
18. Kurita T, Medina RT, Mills AA, Cunha GR. Role of p63 and basal cells in the prostate. Development. 2004; 131:4955–4964. [PubMed: 15371309]
19. Livera G, Petre-Lazar B, Guerquin MJ, Trautmann E, Coffigny H, Habert R. p63 null mutation protects mouse oocytes from radio-induced apoptosis. Reproduction. 2008; 135:3–12. [PubMed: 18159078]
20. McGrath JA, Duijf PH, Doetsch V, Irvine AD, de Waal R, Vanmolkot KR, et al. Hay-Wells syndrome is caused by heterozygous missense mutations in the SAM domain of p63. Hum Mol Genet. 2001; 10:221–229. [PubMed: 11159940]
21. Moll UM, Slade N. p63 and p73: roles in development and tumor formation. Mol Cancer Res. 2004; 2:371–386. [PubMed: 15280445]
22. Petre-Lazar B, Livera G, Moreno SG, Trautmann E, Duquenne C, Hanoux V, et al. The role of p63 in germ cell apoptosis in the developing testis. J Cell Physiol. 2007; 210:87–98. [PubMed: 16998800]
23. Petre-Lazar B, Moreno SG, Livera G, Duquenne C, Habert R, Coffigny H. p63 expression pattern in foetal and neonatal gonocytes after irradiation and role in the resulting apoptosis by using p63 knockout mice. Int J Radiat Biol. 2006; 82:771–780. [PubMed: 17148261]
24. Reis-Filho JS, Milanezi F, Amendoeira I, Albergaria A, Schmitt FC. Distribution of p63, a novel myoepithelial marker, in fine-needle aspiration biopsies of the breast: an analysis of 82 samples. Cancer. 2003; 99:172–179. [PubMed: 12811858]
25. Medawar A, Virolle T, Rostagno P, de la Forest-Divonne S, Gambaro K, Rouleau M, et al. DeltaNp63 is essential for epidermal commitment of embryonic stem cells. PLoS ONE. 2008; 3:e3441. [PubMed: 18927616]

26. Boldrup L, Coates PJ, Gu X, Nylander K. DeltaNp63 isoforms regulate CD44 and keratins 4, 6, 14 and 19 in squamous cell carcinoma of head and neck. J Pathol. 2007; 213:384–391. [PubMed: 17935121]
27. Ihrie RA, Marques MR, Nguyen BT, Horner JS, Papazoglu C, Bronson RT, et al. Perp is a p63-regulated gene essential for epithelial integrity. Cell. 2005; 120:843–856. [PubMed: 15797384]
28. Borrelli S, Candi E, Alotto D, Castagnoli C, Melino G, Vigano MA, et al. p63 regulates the caspase-8-FLIP apoptotic pathway in epidermis. Cell Death Differ. 2008
29. Keyes WM, Mills AA. p63: a new link between senescence and aging. Cell Cycle. 2006; 5:260–265. [PubMed: 16434880]
30. Kurita T, Cunha GR. Roles of p63 in differentiation of Mullerian duct epithelial cells. Ann N Y Acad Sci. 2001; 948:9–12. [PubMed: 11795399]
31. Kurita T, Mills AA, Cunha GR. Roles of p63 in the diethylstilbestrol-induced cervicovaginal adenosis. Development. 2004; 131:1639–1649. [PubMed: 14998922]
32. Suzuki K, Haraguchi R, Ogata T, Barbieri O, Alegria O, Vieux-Rochas M, et al. Abnormal urethra formation in mouse models of split-hand/split-foot malformation type 1 and type 4. Eur J Hum Genet. 2008; 16:36–44. [PubMed: 17878916]
33. Guo X, Mills AA. p63, cellular senescence and tumor development. Cell Cycle. 2007; 6:305–311. [PubMed: 17224650]

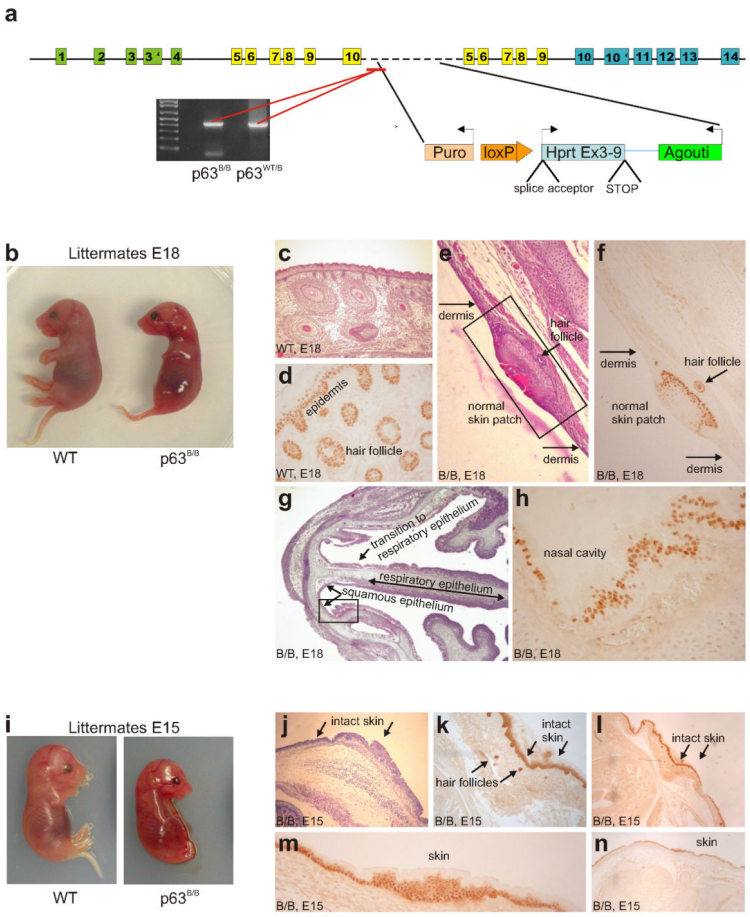

Figure 1. Brdm2 mutant squamous epithelium expresses p63 protein(s)

(a) The targeted Brdm2 allele is shown 2. The pTV12E(60) vector used for the gap repair method of gene ablation of *Trp63* in Brdm2 mice contains an *Agouti* minigene, the 3′ portion of an *hprt* cassette followed by its 3′UTR, a *loxP* site, a puromycin resistance gene, and a 129S5-derived DNA fragment containing *Trp63* exons 5, 6 and 10 4. *Insert* genotyping of our Brdm2/Brdm2 (B/B) mice across the *Trp63* genome/vector border confirmed the insertion of the targeting vector between Exons 10 and 10′ (red line, mutant-specific PCR product). Note: Ex10′ was formerly called Ex15 (see Genbank AF533892).

(b) WT and p63 Brdm2/Brdm2 littermate embryos at day E18.

(c, d) WT embryo at E18. p63 expression in basal and suprabasal cells of skin and hair follicles. **(c)** H&E section. **(d)** Immunoperoxidase staining with p63-specific antibody 4A4. (**d, f, h, k-n)** All 4A4 immunostainings were performed side-by-side, using identical conditions.

(e, f) Microscopically, p63B/B embryos at day E18 exhibit essentially absent epidermis, leaving only underlying compressed dermis. (**e)** H&E. However, rare remnant epidermal patches with relatively normal squamous stratification and hair follicles are present, which **(f)** express p63 in basal and suprabasal cells.

(g, h) In mechanically protected anatomic niches like the anterior nasal cavity, p63B/B embryos at day E18 exhibit normal appearing squamous epithelium that expresses p63. (**g)**

H&E section. (**h**) p63-expressing squamous epithelium lining the vestibulum and lateral nasal cavity. Enlarged view of boxed area in **(g)**. Respiratory epithelium covering the nasal septum is p63-negative (not shown).

(i) WT and p63B/B littermate embryos at day E15. In contrast to mutant E18 embryos which have all but lost their epidermis, mutant E15 embryos do exhibit an - albeit thin and translucent — but completely intact epidermal integument which is visible by eye under 4x magnification.

(**j-n**) Mutant E15 epidermis consists of a contiguous 3-5 cell layer terminally differentiated squamous epithelium with focal thickening and patchy underlying hair follicles, expressing p63 in basal and suprabasal cells. **(j)** H&E sections. **(k-n)** 4A4 immunoperoxidase-stained sections.

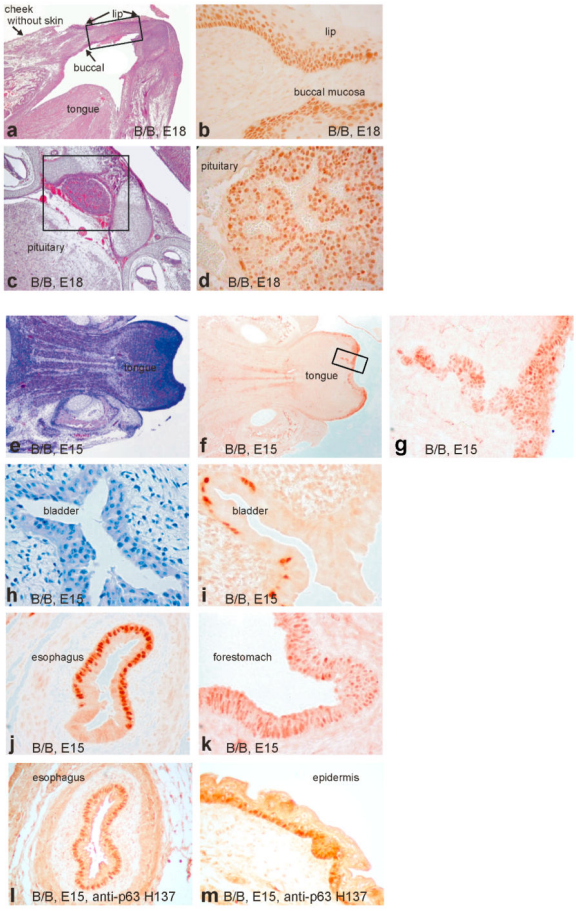

Figure 2. p63 expression in squamous epithelium, pituitary and internal stratified squamous mucosa of Brdm2/Brdm2 embryos

(**a, b**) At day E18, p63 Brdm2/Brdm2 embryos exhibit remnants of normal squamous epithelium that expresses normal levels of p63, particularly in mechanically protected anatomic niches. While cheeks and much of the oral cavity and tongue are denuded at this stage, squamous epithelium is still lining parts of the lip and buccal mucosa.

(**c, d**) p63 Brdm2/Brdm2 embryo at day E18 with normal anterior lobe of the pituitary gland. This glandular epithelium, located in the sella turcica of the skull base and embryologically derived from the oral ectoderm of Rathke's pouch, also strongly expresses p63 in nuclei. (**a, c**) H&E sections. (**b, d**) 4A4 immunoperoxidase staining of areas within the framed H&E sections.

(**e-k**) At day E15, p63 Brdm2/Brdm2 embryos exhibit internal stratified squamous mucosa covering tongue, buccal areas, oropharynx and nasopharynx, esophagus, forestomach and bladder which appears intact by H&E (**e, h**) and express p63 (**f, g, i-k**). 4A4 immunoperoxidase staining.

(**l, m**) Immunoperoxidase staining with pan p63-specific polyclonal H-137 of esophagus and epidermis. E15 p63 Brdm2/Brdm2 embryos.

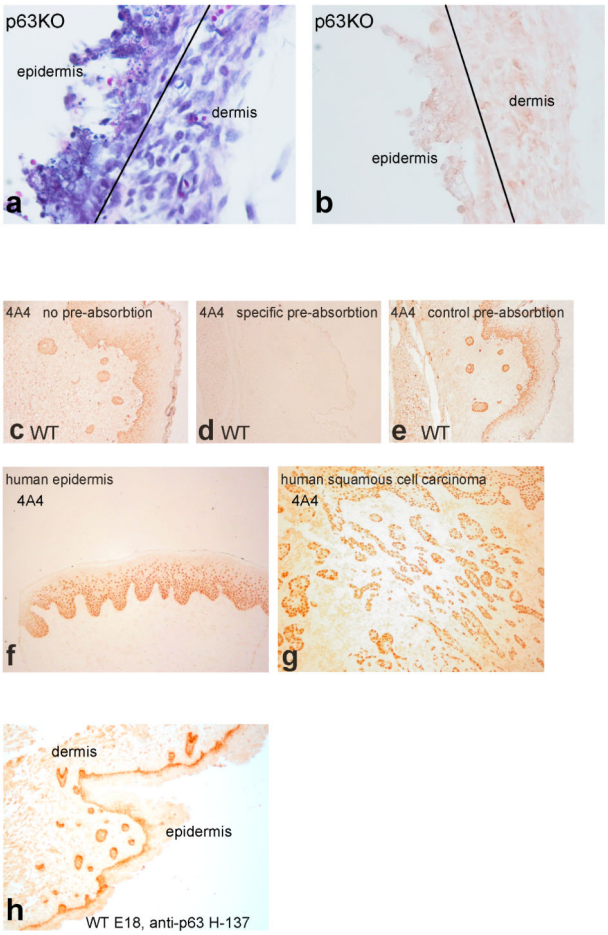

Figure 3. Validation of p63 specificity of classic monoclonal antibody 4A4

(**a, b**) Remnant squamous epithelium from skin of p63 -/- mice (Yang A et al, 1999) at day E17 is devoid of any 4A4 staining. Only non-specific background is detectable.

(**c-e**) Nuclear staining by monoclonal p63 antibody 4A4 is specifically eliminated by p63 proteins. Skin of a WT embryo at day E19, (**c**) stained with 4A4 without pre-absorption, (**d**) 4A4 specifically pre-absorbed with H1299 lysates transfected with a 1:1 mixture of TAp63α and ΔNp63α plasmids (SDS-free, 50-fold excess by total protein w:w), and (**e**) 4A4 that had been control pre-absorbed with empty vector-transfected H1299 lysates (SDS-free, 50-fold excess by total protein w:w). The same amount of 4A4 IgG (2 μg) and conditions were used in all cases. Note that 4A4 staining becomes even sharper with non-specific control pre-absorption. Omitting the primary antibody also eliminated all staining (not shown).

(**f, g**) Specificity validation of 4A4 on human tissue. The antibody stains the same cell types (basal keratinocytes and squamous carcinoma cells) in mouse and human tissues. 4A4 immunoperoxidase staining on sections of normal human skin and invasive squamous cell carcinoma.

(h) Specificity validation of H-137 on E18 WT mouse skin.

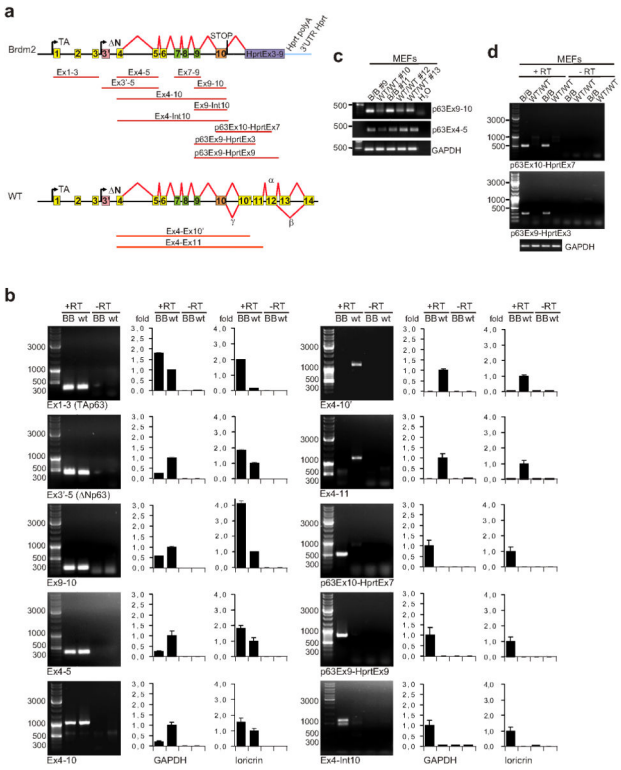

Figure 4. Expression of p63Ex10-truncated transcripts from the Brdm2 allele

(a) Summary of RT-PCR products (red lines) obtained from p63 Brdm2/Brdm2 and WT embryos at day E15. Products obtained only in WT embryos are shown separately (*bottom)*.

(b) Quantitative real-time RT-PCR analysis of p63 transcripts in p63 Brdm2/Brdm2 and WT embryos at day E15. Columns 1-3 show common transcripts, columns 4-6 show unique transcripts. Relative amounts of p63 normalized to GAPDH or loricrin, an epidermal differentiation marker, with WT levels set to 1.0 whenever above zero. Additional normalizations to cytokeratin K5, K10, K14, and desmosome marker PERP confirmed comparable p63 transcript levels between mutant and WT embryos (Supplemental Figure 1 and data not shown). Error bars indicate standard error from three independent experiments. *Columns 1 and 4* qualitatively show the corresponding amplicons after 40 cycles. For controls, PCR reactions on genomic templates not reverse transcribed (-RT) were run. Individual amplicons are indicated.

(c, d) RT-PCR analysis of mouse embryo fibroblasts (passage 5) derived from WT and p63 Brdm2/Brdm2 (B/B) embryos. Transcripts are shown after 40 cycles. GAPDH as input control. Individual amplicons are indicated.

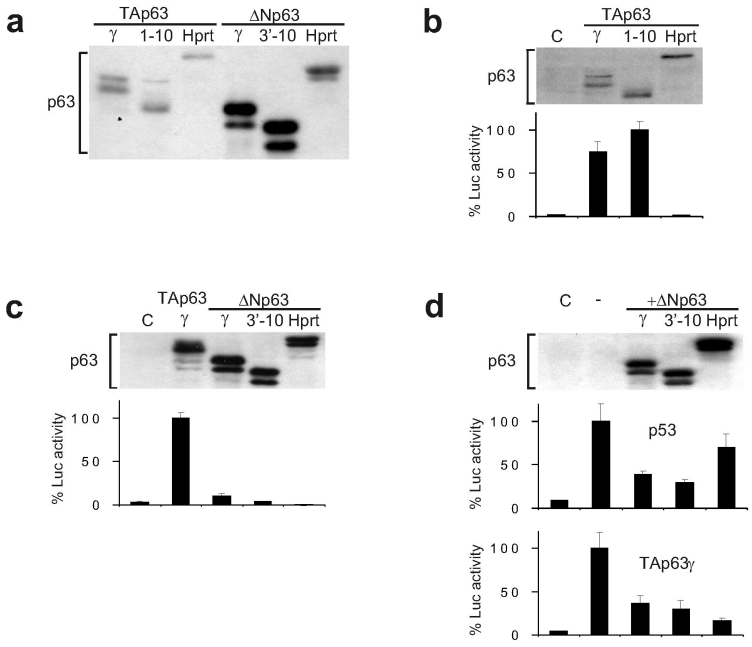

Figure 5. Transcriptional functions of p63Ex10-truncated proteins generated from the Brdm2 allele

(a) Steady state levels of recombinant p63 proteins from the Brdm2 allele. Native mouse p63γ is shown for comparison. All cDNAs were expressed from the same pcDNA3 vector and plasmid amounts. While the TA(1-10) and ΔN(3′-10) p63 proteins have the same steady state levels as the respective p63γ, the HPRT fusion proteins, adding a 173 amino acid tail, are unstable compared to their respective p63γ counterparts. H1299 cells were transfected with 200 μg plasmid each. After 24 hours, the same percent of cell lysates (20 μg per lane) was immunoblotted with 4A4.

(b-c) Transcriptional activity of Brdm2-derived p63 products, compared to native p63γ. Luciferase reporter assays with the p53/p63-responsive human Mdm2 promoter BP100Luc. TA(1-10) and ΔN(3′-10) behave indistinguishably from genuine p63γ. Hprt-fusion proteins are inactive as transactivator, while ΔN(3′-10)Hprt functions partially as transrepressor of TAp63γ and p53. **(b-c** *bottom***)** Transactivation by the indicated p63 proteins. Respective protein amounts shown by 4A4 immunoblot in **(b-c** *top***).**

(**d**) Transrepression of co-expressed p53 or TAp63γ by the indicated p63 proteins, shown on top**.** Plasmid amounts were adjusted to obtain equal protein expression of the various p63 proteins.

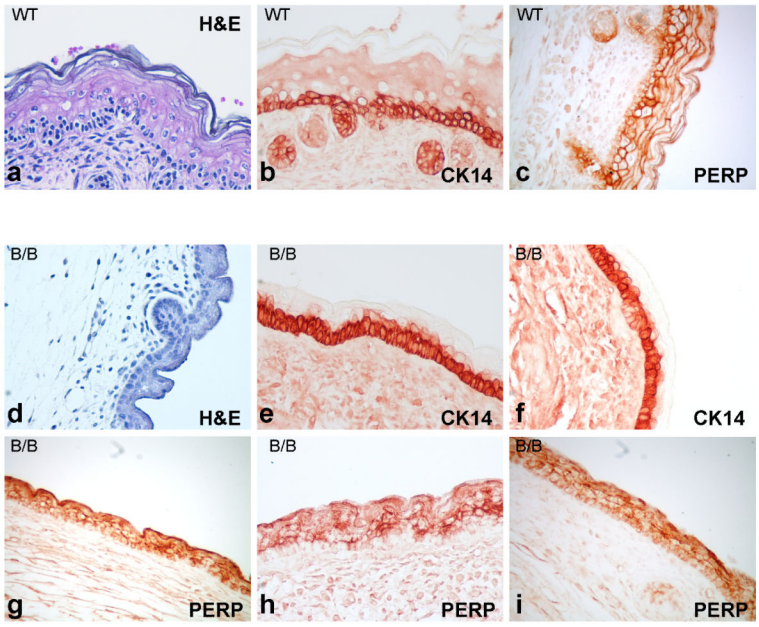

Figure 6. Expression of CK14 and PERP, important bona fide epidermal target genes of p63γ, in E15 Brdm2/Brdm2 embryos

Skin of WT embryos at day E18 (**a-c**) and skin of Brdm2/Brdm2 embryos at day E15 (**d-i**) express CK14, a marker of the basal layer of stratified epithelia and PERP, a component of desmosomes. Immunoperoxidase staining.